Discrete modelling of continuous dynamic recrystallisation by modified Metropolis algorithm

Computational Materials Science 234 (2024) 112804

Contents lists available at ScienceDirect

Computational Materials Science

journal homepage: www.elsevier.com/locate/commatsci

Full length article

Discrete modelling of continuous dynamic recrystallisation by modified Metropolis algorithm

Siying Zhu *, Elijah Borodin, Andrey P. Jivkov

Department of Solids and Structures, School of Engineering, The University of Manchester, Manchester M13 9PL, UK

ARTICLE INFO

Keywords:
Copper alloys
Equal-channel angular pressing
High-pressure torsion
Severe plastic deformation
Metropolis algorithm
Continuous dynamic recrystallisation
Grain boundaries
Algebraic topology

ABSTRACT

Continuous dynamic recrystallisation (CDRX) is often the primary mechanism for microstructure evolution during severe plastic deformation (SPD) of polycrystalline metals. Its physically realistic simulation remains challenging for the existing modelling approaches based on continuum mathematics because they do not capture important local interactions between microstructure elements and spatial inhomogeneities in plastic strain. An effective discrete method for simulating CDRX is developed in this work. It employs algebraic topology, graph theory and statistical physics tools to represent an evolution of grain boundary networks as a sequence of conversions between low-angle grain boundaries (LAGBs) and high-angle grain boundaries (HAGBs) governed by the principle of minimal energy increase, similar to the well-known Ising model. The energy is minimised by a modified Metropolis algorithm. The model is used to predict the equilibrium fractions of HAGBs in several SPD-processed copper alloys. The analysis captures non-equilibrium features of the transitions from sub-grain structures to new HAGB-dominated grain structures and provides estimations of critical values for HAGB fractions and accumulated strain at these transitions.

1. Introduction

Severe plastic deformation (SPD) can significantly improve the strength of alloys by reducing their grain size [1–3]. Typically, SPD refines grains and reduces an average grain size to the sub-micron scale by creating new high-angle grain boundaries (HAGBs), i.e., by increasing the HAGB fraction in the resulting polycrystalline structure [4,5]. Several SPD processing techniques have been developed to produce ultrafine-grained (UFG) materials. Those of largest industrial interest include [6]: equal channel angular pressing (ECAP) [7,8]; high-pressure torsion (HPT) [9], including ECAP-Conform [10,11]; multi-directional forging (MDF) [12]; and accumulative roll bonding (ARB) [13]. In particular, the HPT methodology is found to be efficient for creating UFG structures with grains down to several nanometres with predominantly HAGBs [14], while ECAP allows for manufacturing relatively large cylindrical samples with outstanding mechanical properties without significantly changing the shapes and sizes of the samples [6,15].

Dynamic recrystallisation (DRX) [16] is the dominant mechanism of grain refinement during SPD [4]. It has been shown that both continuous (CDRX) and discontinuous (DDRX) recrystallisation can contribute to the microstructure evolution during SPD [4,5]. At relatively low temperatures and high strain rates, CDRX [16,17] becomes the primal recrystallisation mechanism in copper alloys [18]. CDRX is shown schematically in Fig. 1. At very small plastic strains clusters with a high density of dislocations are formed (Stage 1). As the deformation develops, these clusters evolve into dislocation walls, which form sub-grains. The dislocation walls are low-angle grain boundaries (LAGBs) with crystallographic misorientations smaller than the commonly accepted threshold value of 15 degrees [19] (Stage 2). After this stage, sub-grain structures with a large fraction of LAGBs are formed [5]. Further deformation promotes the rotation of the sub-grains (Stage 3). Eventually, the majority of the formed LAGBs convert to HAGBs, i.e., grain boundaries with crystallographic misorientations larger than 15 degrees. At the final Stage 4 of the CDRX process, a dynamic balance between the formation of new LAGBs and their conversion into HAGBs is achieved [20,21]. After this final stage, the new UFG structure with a large fraction of HAGBs is formed, and the new grains can be distinguished from the initially created dislocation cells structure at Stage 2. It is challenging to establish when the new grain microstructure appears and which event in the microstructure evolution marks the transition between the last two stages. It is natural to consider that a percolation of the HAGB network is the critical event [19,22]. The network percolation, however, is not a well-defined characteristic since it could be size and orientation-dependent. It is desirable to explore other descriptors that are intrinsic to the microstructure, e.g., based on relations between different grain boundary types, and correlate these with the macroscopic strain.

* Corresponding author.
E-mail addresses: siying.zhu@manchester.ac.uk (S. Zhu), elijah.borodin@manchester.ac.uk (E. Borodin), andrey.jivkov@manchester.ac.uk (A.P. Jivkov).

https://doi.org/10.1016/j.commatsci.2024.112804
Received 17 May 2023; Received in revised form 10 January 2024; Accepted 11 January 2024

List of Symbols

S	Configurational entropy
j_i	Fraction of i-type triple junctions
q_i	Fraction of i-type quadruple nodes
p	Fraction of high angle grain boundaries
ε_p	Equivalent plastic strain
W	Plastic work during the continuous dynamic recrystallisation
w	Energy spent on destruction of the system order
σ_y	Yield stress
ε	Accumulated plastic strain
η	Fraction of the total plastic work stored in the form of new defect structures
ν_i	Spins in the Ising model
$\mathcal{H}$	Hamiltonian of the Ising model
ω_i	Topological weight of the ith grain boundary
u	Distortional strain energy
h	Energy density $h = \zeta \cdot u$
Π^{acc}	Acceptance probability in Metropolis algorithm
p_L	Probability of conversion of low to high angle grain boundary
b	Burgers vector of dislocations
ρ_D	Average scalar dislocation density
d	Average grain size of material
α, ζ, g	Ising model parameters

The existing approaches to modelling microstructure evolution belong to two classes [23,24]: continuum-based and meso-structural. In continuum-based approaches, the microstructure evolution is described by a set of internal state variables [25,26], while the elastoplastic deformation is described in a classical continuum mechanics manner [27–29]. The use of continuum-based approaches dominates the engineering papers [30,31]. Their advantage is the simplicity in obtaining the average macroscopic behaviour of materials with dynamically changing microstructures. Since the solutions use finite element analysis, they are considered the most practical for mechanical engineers at present. However, the continuum-based approaches come with several limitations. First, the incorporation of texture-related parameters affecting the mechanical behaviour of a material, such as grain orientations and grain boundary misorientations, is challenging. Second, analysis of size effects is impossible without introducing higher-order theories, e.g., strain-gradient plasticity and the associated difficulty with calibrating their parameters. Third, interactions between microstructural elements of different dimensions, such as grains, grain boundaries and triple lines, cannot be taken into account [32]. As a result, the continuum-based approaches alone are not appropriate for the correct description of the CDRX phenomenon and related strain hardening [28] of material; an explicit account of the finite, discrete nature of the microstructure is required.

On the other side, the mesoscale structural approaches reflect the discrete nature of the materials' microstructures or, as a minimum, account for existing discontinuities [33,34]. These include Monte-Carlo models [35–37], cellular automata [35,37,38], vertex or front tracking models [39,40], level set models [41,42], and phase field models [43,44]. The listed discrete approaches have different application domains, but none offer the possibility to relate elements with different dimensions and investigate the topological properties of the corresponding networks. It is, therefore, necessary to develop a modelling approach that captures the distribution and connectivity of different microstructural elements and provides a suitable framework for their topological analysis.

Building on the recent theoretical developments of fully discrete representation of grain boundary and triple junction networks and their evolution during SPD [45,46], the present work investigates potential governing principles of CDRX by explicitly studying transitions between LAGBs and HAGBs. The polycrystalline materials are represented by polyhedral assemblies constructed by Voronoi tessellations of three-dimensional (3D) regions [47]. These resemble real materials' microstructures [48,49], and are described in Section 2. The polyhedral assemblies are geometric realisations of cell complexes in algebraic topology. The description of such complexes provides complete information about the connectivity between structural elements of different topological dimensions. The proposed approach allows for the analysis of all sub-structures formed by grains, grain boundaries (LAGBs and HAGBs), and triple junctions of different types. The classical Ising model is therefore adapted to describe the structure evolution. This is discussed in Section 3 together with the numerical implementation — the Metropolis algorithm [50]. Section 4 presents the application of the developed discrete cell complex methodology and the proposed governing principle to study grain structure evolution during ECAP and HPT processing of copper alloys.

2. Discrete model of microstructure evolution during CDRX

An optimised Laguerre–Voronoi tessellation, provided by an open-source software *Neper* [47], is used in this work. The Voronoi polyhedrons represent grains or subgrains. They are convex and bounded by polygonal faces representing grain or subgrain boundaries (GBs). Three polyhedrons share a common edge, which represents a triple line/junction (TJ). Four polyhedrons meet at a point called quadruple point/node (QN). The sets of grains or subgrains, GBs, TJs, and QNs are sub-structures of the polycrystalline assembly with elements of geometric dimensions 3D, 2D, 1D, and 0D, respectively. In the language of algebraic topology, such an assembly is a polytopal cell complex (PCC) denoted by $\mathcal{M}$. A k-cell in $\mathcal{M}$ represents a vertex, an edge, a polygonal face and a polyhedron for $k = 0, 1, 2, 3$, respectively; this is illustrated in Fig. 2(a).

The model used in this work considers a binary classification of GBs — LAGBs and HAGBs. It has been observed with different materials that a given accumulated strain during CDRX the fractions of LAGBs and HAGBs reach equilibrium. The balance of LAGBs and HAGBs is analysed in the present work by mapping the 3D grain boundary network to a graph, on which the Ising model is applied.

Configuration entropy is a useful descriptor of materials' microstructure topology encoding the amount of information associated with the specific defect microstructure. The configuration entropy, defined in [46,51] and used in [32,45], is based on the fraction of different types of TJs and can be calculated during the evolution process by [45]:

$$S = -\sum_{i=0}^{3} j_i \log_2 j_i. \tag{1}$$

where $j_i = N_i / \sum N_i$ are the ratios between the number of TJs $N_i (i \in [0, 1, 2, 3])$ of type $J_i (i \in [0, 1, 2, 3])$ and the total number, $N = \sum N_i$, of TJs in the discrete cell complex.

A 3-cell of $\mathcal{M}$ fully bounded by HAGBs is considered a grain. A 3-cell of $\mathcal{M}$ with one or several LAGBs on its boundary is considered a subgrain [8]. The CDRX process leads to a significant increase in the HAGB fraction p up to 0.7–0.9 [4] at large plastic strains. This means that there is a higher probability of getting more grains at higher strains. Different experimental conditions and processes will affect the recrystallisation rate and the final fraction of HAGBs [4,18]. The simulations start with an arbitrary grain boundary network, in which the LAGBs and HAGBs are randomly assigned. For the modified Ising model described in

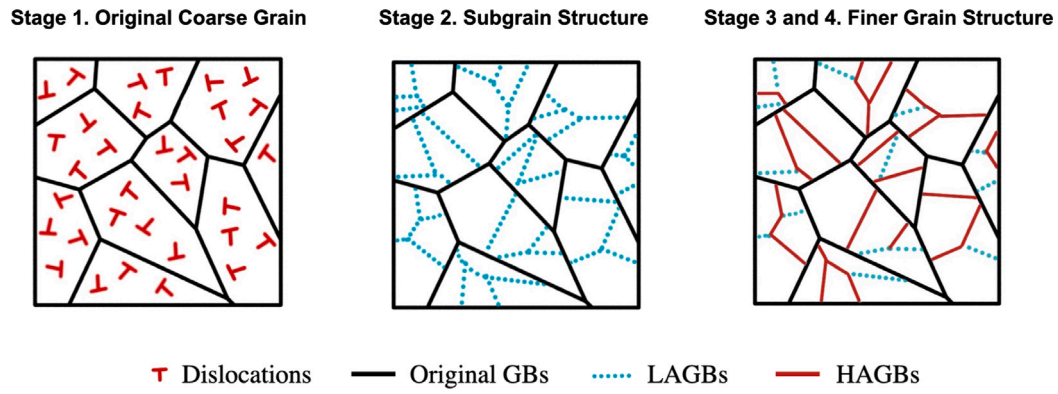

Fig. 1. Schematic representation of four different stages of CDRX process.

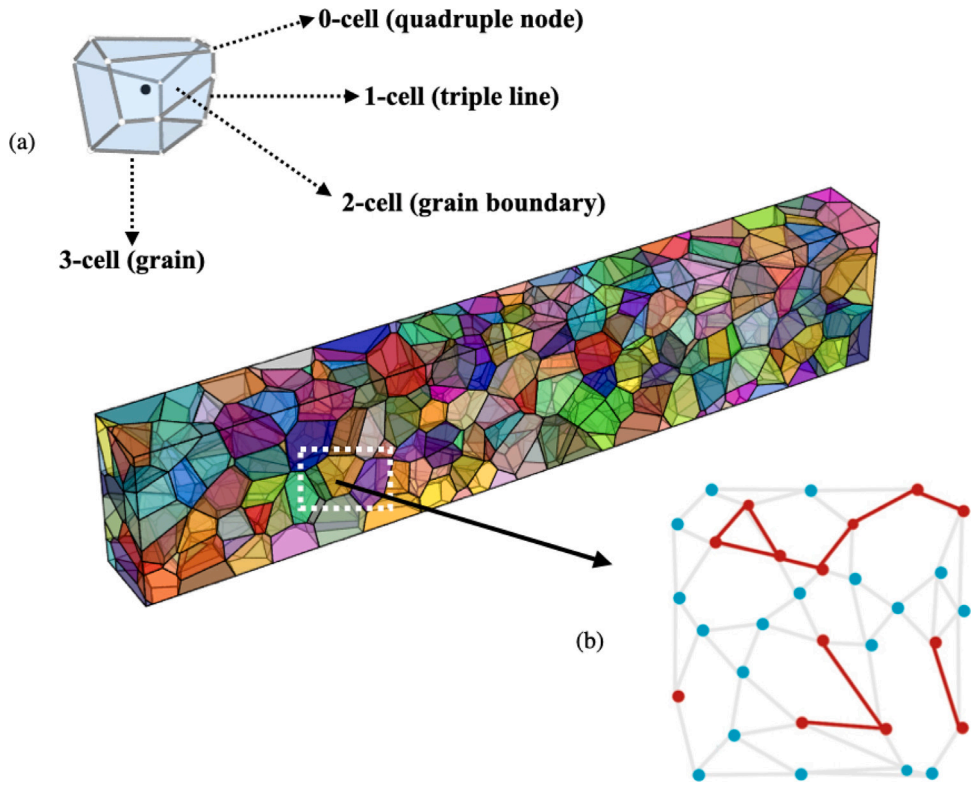

Fig. 2. (a) Cells of a 3-complex with different topological dimensions; (b) Graph representation of GB networks: Grain boundaries are graph nodes - blue nodes are LAGBs, red dots are HAGBs; Grain boundaries sharing TJs are connected by graph edges - grey edges form LAGBs network, red edges form HAGBs network.

Section 3, different plastic strain values are used as input, and various parameters (material and experimental process related) act together in the iterative process, leading to the equilibrium state.

Practically, at small plastic strains around $\varepsilon_p \approx 0.3$, the initial coarse-grained structure has been transformed into a system of sub-grains by creating a large number of dislocation walls [45] (see Stage 2 in Fig. 1). The simulation, therefore, covers the part of the CDRX process where the former LAGBs are being converted into new HAGBs, typically by sub-grain rotations (see Stage 3 in Fig. 1). The aim of this work is to find the equilibrium state at every plastic strain level.

3. Modified Ising model

The tendency of a system in equilibrium to have minimal total energy is a fundamental principle commonly used in physical sciences. The binary classification of GBs allows for exploiting a well-known binary Ising model used extensively in statistical mechanics for investigating phase transition in very different physical systems [52] – from dynamics of magnetic spin systems to evolution of grain boundaries [53,54]. It was first proposed in 1920 by Wilhelm Lenz [55], then solved in one dimension by his Ph.D. student Ernst Ising [56]. The model defines a Hamiltonian [56] and provides the probability distribution of the possible macroscopic states of a system whose elements can be in two distinct microscopic states traditionally referred to as spins. For applying the Ising model, the GB network is represented by a graph, where the GBs are graph nodes and GBs with common triple junctions are connected by edges; this is illustrated in Fig. 2(b).

The essential components of the Ising model are temperature and Hamiltonian, which is the total energy associated with the system elements in the presence of the external field. By definition, the temperature is a derivative of energy with respect to entropy. In many cases, the relation between the temperature and the Hamiltonian parameters, strengths of external fields h_i and interactions g_{ij}, is negligibly weak compared to the relation between the temperature and the system disorder measured by the entropy [57]. Increasing the temperature

to infinity ultimately destroys any order, creating a wholly stochastic arrangement of the system elements. For the considered CDRX process, the plastic strain ε is a direct analogue to the thermodynamic temperature, as argued below.

The simulations start at the CDRX Stage 2 (see Fig. 1) when the sub-grain structure is already formed, and the HAGB fraction is very small, about 5%. This LAGBs-dominated structure has minimal possible energy, which can only increase due to the creation of new HAGBs. In the following Stages 3 and 4 (Fig. 1), the plastic deformation acts against the elastic forces, creating a meta-stable HAGB structure. At Stage 4, according to the model of rotational DRX [58], nearly equiaxed grains covered mostly by HAGBs became elongated during deformation. This causes the creation of several new LAGBs or dislocation walls inside elongated grains. The LAGBs are converted into new HAGBs by means of subgrains' rotation mechanism [58]. New equiaxed grains are created, and the process of elongation-subdivision is repeated. Along with this process, arbitrary grain rotations occur because of the inflow of dislocations into grain boundary and reverse diffusion processes [59]. As a result, the plastic deformation ultimately destroys any special ordering in grain orientations. It leads to a large fraction of HAGBs, but the final state strongly depends on the elastic modulus of the material and the material's yield stress. This suggests that during CDRX the cold plastic work $W = \sigma_y \cdot \varepsilon$, where σ_y is the yield stress, plays a role similar to the thermal energy in the ferromagnetic materials. More precisely, only a fraction of the total plastic work $\eta \sim 0.1$ is stored in the form of new defect structures [60], while the rest is dissipated as heat. Hence, the energy spent on the destruction of the system order is:

$$w = \eta \cdot \sigma_y \cdot \varepsilon. \tag{2}$$

Contrarily, the Hamiltonian drives the system towards the maximum possible order at a given temperature/plastic strain, e.g., the creation of a HAGBs-dominated structure after CDRX. The presence of an external field selects preferred spins that form the configuration with the lowest possible total energy. From the grains perspective, the Hamiltonian is minimised by minimising the stored elastic energy in grains. The elastic energy in a grain is $U = \sigma^2/C$, where C is elastic modulus dependent on the grain orientation with respect to the direction of the externally applied force. There is an optimal grain orientation corresponding to minimum elastic energy. A grain with a non-optimal orientation, i.e., storing larger than the minimum energy, will have the tendency to rotate to reduce the stored energy to the minimum. The critical stress for conversion can be estimated from the local energy balance $\sigma_{cr}^2/C \cdot d^3 \approx \Delta\gamma_{gb}\delta d^2$, where $\Delta\gamma_{gb}$ is the increase of grain boundary excess energy after conversion from LAGB to HAGB, $\delta \approx 1$ nm is the grain boundary thickness and d is the grain size. As the grain boundary energy differences in alloys are about 1 J/m^2, the critical stress σ_{cr} is much smaller than the yield stress in nanocrystalline materials. This means that rotations might occur prior to macroscopically observed yielding.

According to the DRX mechanism, the elongated grains with nearly optimal orientation create several new sub-grains bounded by LAGBs. Rotations of sub-grains are necessary for turning their LAGBs into HAGBs that must increase the elastic energy. The larger the external force, the larger the change of elastic energy in a sub-grain due to its rotation. It is assumed here that this process of elastic energy increase is more common in the developed CDRX process during SPD than the minimisation of elastic energy natural for the initial stages of plastic deformation. The external force for rotation is the von Mises stress, which is proportional to the second invariant of the deviatoric stress tensor. During SPD, this stress can be assumed equal to the current yield stress of the material, s_y. In such a case, the creation of new HAGBs requires an increase of energy proportional to the distortional strain energy, given by:

$$u = s_y^2/2\mu, \tag{3}$$

where μ is the shear modulus of the material. In addition to the effect of stresses, which are viewed as the external field in the Ising model, GB interactions can also be taken into account to represent the possibility that the neighbourhood of a given GB can facilitate its conversion from LAGB to HAGB, decreasing the potential barrier needed for such conversion.

Consider a graph $G = (V, E)$, such that the elements of V correspond to the GBs of a given polycrystalline assembly, and the elements of E correspond to pairs of GBs that have a common triple line/junction in the assembly. The construction of this graph is unique and provides the structure for the Ising model. The spins associated with the vertices correspond to the two GB types: -1 is assigned to vertices representing LAGBs, and $+1$ is assigned to vertices representing HAGBs. The Hamiltonian for the modified Ising model is given by:

$$\mathcal{H} = -\sum_i \omega_i h v_i - \sum_{e_{ik}} g \cdot h(\omega_k/\omega_i) v_i v_k, \tag{4}$$

here ω_i is the topological/combinatorial weight [61] of the GB corresponding to vertex i, and the energy density h is given by:

$$h = \zeta \cdot u, \tag{5}$$

where ζ is a constant, and u can be calculated by Eq. (3). The interaction term uses a parameter $g \geq 0$, which scales the energy density h to define an interaction strength with existing HAGBs only, i.e., the summation is over the edges connecting the current GB i with neighbouring HAGBs k. In the absence of HAGB neighbours, the interaction term is zero. The combinatorial weights ω_i of cells of different dimensions in a cell complex have been proposed in [61] for calculating combinatorial curvatures. In that proposal, the weight of a 2-cell equals the number of 1-cells on its boundaries, which is half the number of neighbouring 2-cells. In the present work, the weight of a grain boundary equals the number of neighbouring GBs. This means that each vertex in G is assigned a weight equal to the number of edges in G adjacent to the vertex. It can be shown [62] that for the Voronoi tessellation of space, the GB weight is proportional to the GB area, so the large weights correspond to the large GBs. Thus, the weights qualitatively represent that the larger boundaries with a large number of neighbours require a larger amount of energy for their conversion into HAGBs. The weights w_k in the interaction terms reflect the slight effect from the side of the small neighbouring GBs compared with the large ones.

The assignment of $v_i = +1$ spin for all HAGBs and $v_i = -1$ spin for all LAGBs, makes the conversion from HAGBs to LAGBs energetically favourable, and the external field s_y facilitates such conversions. Concurrently, the Hamiltonian energy (Eq. (4)) acts as a potential barrier for LAGB to HAGB conversions because it increases with increasing s_y or decreasing μ in Eq. (3), which prevents the formation of new HAGBs. The presence of HAGBs in a GB neighbourhood introduces spins $v_k = -1$ in the interaction term sum, which leads to a decreasing Hamiltonian. The more the HAGBs in the neighbourhood and the larger the interaction energy ratio g, the less the potential barrier for LAGBs to HAGBs conversion. At $g > 1$, once the number of neighbouring HAGBs becomes larger than the number of LAGBs, the term $|\sum_k g \cdot (\omega_k/\omega_i) v_k| > \omega_i$ (as $max\left(|\sum_k v_k|\right) = \omega_i$) and the LAGBs to HAGBs transition becomes energetically favourable ($\Delta H < 0$) for all $\omega_k \sim \omega_i$. The existence of large neighbouring grains with adjacent HAGBs ($\omega_k \gg \omega_i$) have the same effect and make conversion energetically favourable.

3.1. Metropolis algorithm for energy minimisation

To simulate the process of structure evolution, one can implement the Monte Carlo random process numerically. The Monte Carlo simulations follow a Markov chain, which is completely specified by the transition probability matrix Π_{AB} that is the probability of transition to state B in the next step if the current state is A. All Monte Carlo methods follow a simple sequence of steps: (1) generate a pseudo-random number; (2) select items from the current state and try to

transform these to transition to a new state; (3) accept or reject the trial based on the random number and the trial acceptance probability; (4) update the state if the trial is accepted and repeat the process. In the modified Metropolis algorithm, the acceptance probability is given by:

$$\Pi^{acc} = \exp\left(-\frac{\Delta\mathcal{H}}{w_k}\right), \tag{6}$$

where w_k is the part of the plastic work given by Eq. (2). The same values h and g for all grains lead to the following equation for the energy difference, which is used later for calculations:

$$\Delta\mathcal{H} = 2h\nu_m \cdot \left(\omega_m + \frac{g}{\omega_m}\sum_n \omega_n\nu_n\right), \tag{7}$$

where ν_m represents the selected element's spin and ν_n are the spins at the nearest neighbours of that vertex. If $\Delta\mathcal{H} \le 0$, the trial is accepted with $\Pi_{acc} = 1$, otherwise when $\Delta\mathcal{H} > 0$, the trial is accepted with the acceptance probability

$$\Pi^{acc} = \exp\left(-\frac{(s_y^2)_k \cdot (\omega_m + g/\omega_m \sum_n \omega_n\nu_n)}{\mu \cdot \eta(\sigma_y)_k\varepsilon_k}\right). \tag{8}$$

Here $(s_y)_k$ is the yield stress in a single grain independent of the grain boundary structure, while the term $(\sigma_y)_k$ is the average yield stress in the polycrystalline material, and ε_k is a plastic strain. All parameters are taken at simulation step k. If strain hardening is neglected and constant values of stress are assumed, the equation takes the simple form:

$$\Pi_{acc} = \exp\left(-\frac{\zeta' \cdot (\omega_m + g/\omega_m \sum_n \omega_n\nu_n)}{\varepsilon_k}\right), \tag{9}$$

where $\zeta' = s_y^2/(\eta\mu\sigma_y) < 1$ is a constant.

This approach gives $\Pi_{acc} \approx 1$ for very large values of ε_k, which means that both the LAGBs to HAGBs transitions and their reverses are accepted with equal probabilities. That inevitably leads to fractions 0.5 for both boundary types, which does not correspond to the experimental data for HAGB fraction at high accumulated strains [8,45,46]. The problem can be overcome by introducing an additional probability p_L that accounts for the asymmetry between the LAGBs to HAGBs transitions and their reverses. Such asymmetry can be easily explained: the LAGBs, by definition, are boundaries with misorientations between 0 and 15 degrees, while HAGBs are boundaries with misorientations between 15 and 62 degrees for crystals with cubic symmetries. In such case, during grain rotations, the probability for a boundary to become HAGB is $p_L \approx 1 - 15/62 \approx 0.76$. From the other side, p_L physically depends on the "saturation level" in the dislocations density ρ_D^{max}, which is a function of the dislocation annihilation and generation rates (see the following Section 3.2). This means it is a function of the material's purity and defect microstructure. According to materials' characterisation data after SPD [8,18,46], p_L can vary in the range from 0.6 to 0.9, depending on the material and SPD processing route. These considerations lead to the following modified expression for the acceptance probability:

$$\Pi_{acc} = \begin{cases} p_0, & \text{if } \Delta\mathcal{H} \le 0. \\ p_0 \exp\left(-\frac{(s_y^2)_k(\omega_m + g/\omega_m \sum_n \omega_n\nu_n)}{\eta\mu(\sigma_y)_k\varepsilon_k}\right), & \text{if } \Delta\mathcal{H} > 0. \end{cases} \tag{10}$$

where p_0 is related to p_L as follows:

$$p_0 = \frac{\nu_i + 1}{2} - \nu_i(1 - p_L). \tag{11}$$

The steps of the modified Metropolis algorithm become:

1. Start with an arbitrary spin configuration $\{\nu_i\}, \nu_i = \pm 1$;
2. Randomly select a vertex with spin ν_i;
3. Flip the spin, i.e., $\nu_i := -\nu_i$ (trial) and compute the energy change, $\Delta\mathcal{H}$;
4. If $\Delta\mathcal{H} \le 0$, accept the trial with probability p_0 and go to step 6.
5. Else accept the trial with probability $\Pi_{acc} = p_0 \cdot \exp(-\frac{\Delta\mathcal{H}}{w_k})$; if rejected flip the spin back $\nu_i := -\nu_i$;
6. Return to step 1 unless a maximum number of iterations is reached (see Fig. 3).

3.2. Strain hardening model

Strain hardening is essential for many mechanical processes, including SPD, and often cannot be neglected in calculations. The modified Ising model presented in this section contains two different stress-related parameters: the deviatoric stress s_y, representing the local yield stress in a grain, and σ_y representing average yield stress in the whole polycrystalline assembly [28,29,63]. The former depends on the crystallography and the presence of dislocations inside a grain. Using the well-known Taylor and Hall–Petch laws for strain hardening, the following expressions are used [18,59]:

$$s_y = \sigma_y^0 + \alpha\mu b\sqrt{\rho_D}, \tag{12}$$

and

$$\sigma_y = \sigma_y^0 + \alpha\mu b\sqrt{\rho_D} + \frac{K_{HP}}{\sqrt{d}}. \tag{13}$$

Here σ_y^0 is the yield stress of a dislocation-free nanocrystalline sample, $\alpha \approx 0.4$ is the Taylor constant, b is the Burgers vector of dislocations [60], ρ_D is the average scalar dislocation density [28], K_{HP} is the Hall–Petch coefficient [64] and d is the average grain size of material.

A simple approximation for the evolution of dislocation density during SPD shown in Fig. 4(a), can be given by [18,65]:

$$\rho_D = \rho_D^{max}\left[1 + (r_D - 1) \cdot \exp(k_a(r_D - 1) \cdot \varepsilon)\right]^2, \tag{14}$$

where $r_D = \sqrt{\rho_D^0/\rho_D^{max}}$, and $\rho_D^{max} = (\delta_f/k_a b)^2$ is the saturation level or maximal possible dislocation density with the dislocation annihilation coefficient $k_a = 1.9$ [18], dislocation generation parameter $\delta_f \approx 0.01$ [28,63] and the Burgers vector for copper alloys which can be taken equal to $b = 0.256$ nm; ρ_D^0 is the initial dislocation density. The development of dislocation density during SPD depends weakly on the initial dislocation density. The initial value selected here is 10^{11} m^{-2}, which is an average value for copper alloys.

The third term in Eq. (13) contains an average grain size d, which depends on the fraction of HAGBs p [18,65]. It can be estimated as [18]:

$$d = \frac{\beta}{p \cdot \sqrt{\rho_D}}, \tag{15}$$

where the coefficient $\beta \approx 11$ is taken from the dislocation theory [18]; the corresponding result is shown in Fig. 4(b).

4. Results

The principal advantage of the developed discrete approach is that it allows for studying topological changes and accounts for interactions in the grain structure of industrially processed materials. Describing the changes in the HAGB network can provide essential information about the driving forces of the microstructure evolution process. At the same time, energy minimisation as a governing principle is physically correct for the systems close to their equilibrium state; this is often not the case for some highly non-equilibrium SPD processes. At the same time, one fundamental feature of the critical phenomena makes some calculation results based on this model relevant for a much wider range of system evolution routes. The Ising model explicitly addresses the critical behaviour of a system described as a second-order phase transition: when the microscopic parameter p is close to a critical value (percolation threshold) $p = p_c$, the behaviours of all related macroscopic characteristics C_p are described by power laws in the form $C_p \sim (p - p_c)^{-\nu}$ with some power ν. Only the critical

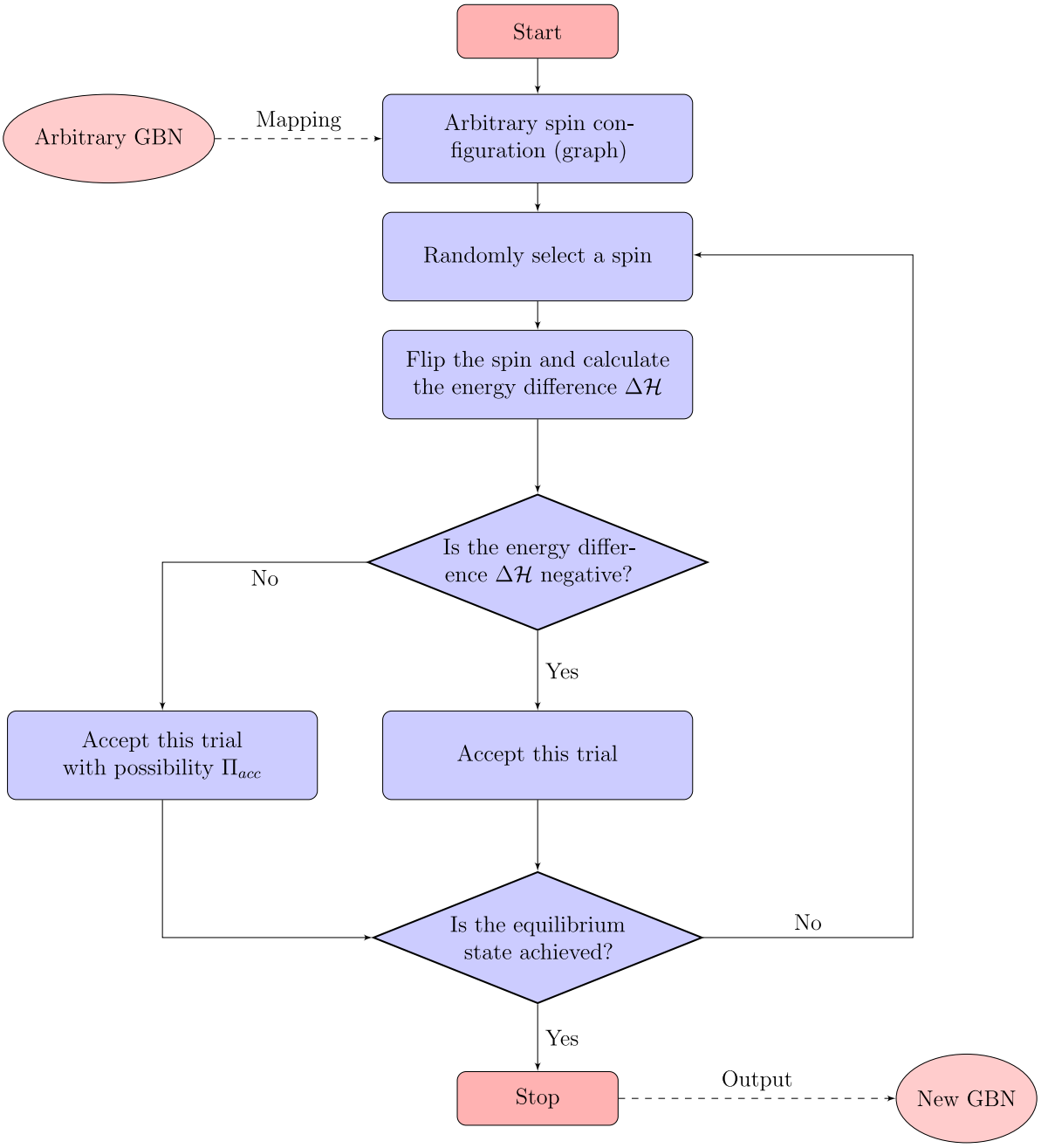

Fig. 3. Modified Metropolis algorithm for generating new grain boundary network.

value p_c here depends significantly on the specific HAGBs arrangement or evolution principle as discussed in [66], while all the coefficients in these power laws are entropy-independent. This makes the Ising-like energy minimisation model useful for obtaining $p(\varepsilon)$ relations, despite its inability to provide the correct spatial distribution of HAGBs. So the developed in the previous sections discrete methodology can be effectively applied for simulations of structure evolution at severe plastic deformation processes like ECAP and HPT.

4.1. ECAP processing of copper alloys

During ECAP, external forces press metallic billets through the L-shaped die with angles between 60° and 135°, but most commonly 90°. This process is repeated many times, leading to large accumulated plastic strains causing a DRX process inside initially coarse grains. After several passes, the ECAP produces UFG materials with an average grain size of about a few hundred nanometres [67].

A cell complex corresponding to a volume of ECAP-processed copper alloy has been created by the software *Neper* [47], as shown in the middle of Fig. 2. A purpose-built Matlab code, implementing the Metropolis algorithm for the modified Ising model, was used for the simulation of HAGBs fraction evolution, as well as for the calculation of the configuration entropy.

Fig. 5(a) shows the experimental [8,68–70] (symbols) and calculated (curves) evolution of HAGBs fractions with accumulated strain for ECAP-processed copper alloys Cu-2%Co, technical purity Cu, oxygen-free Cu and Cu-0.1%Cr-0.06%Zr. The curves are obtained by fitting the Ising model parameters. Fig. 5(b) shows the configuration entropy [45] as a function of the accumulated strain.

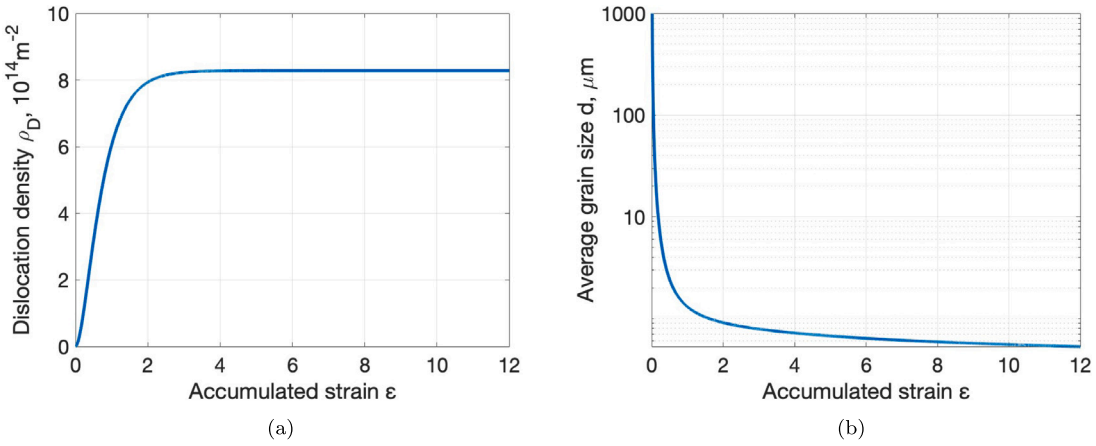

Fig. 4. Dislocation density (a) and average grain size (b) as functions of the accumulated strain during SPD.

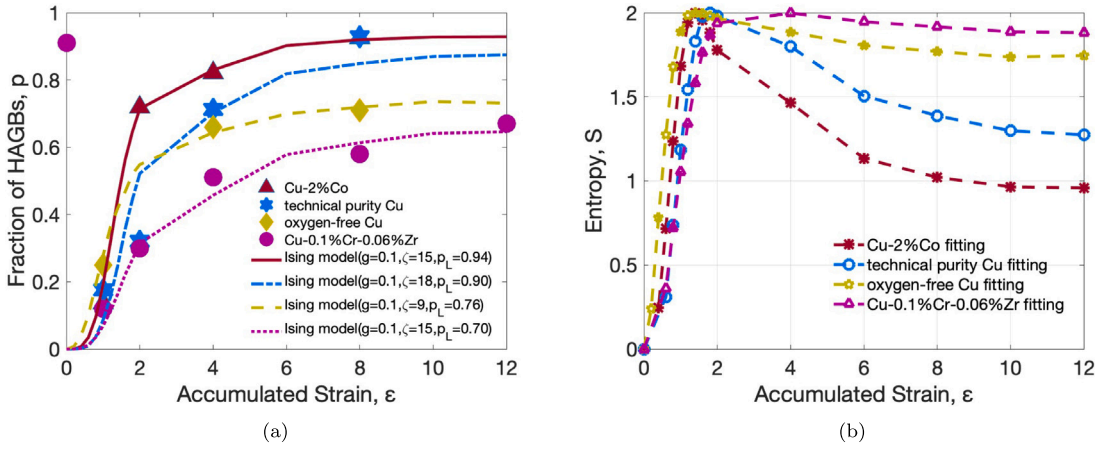

Fig. 5. (a) Comparison of simulated evolution of HAGBs fraction with experimental data on ECAP-processed copper alloys (Cu-2%Co [68], technical purity Cu [69], Cu-0.1%Cr-0.06%Zr [8], oxygen-free Cu [70].); (b) Configurational entropy as a function of accumulated plastic strain during ECAP.

It can be seen from Fig. 5(a) that p_L has the largest effect on the $p-\varepsilon$ dependence. This is best observed by comparing the results for Cu-2%Co and Cu-0.1%Cr-0.06%Zr since g and ζ for these alloys are equal. The value of p_L limits not only the maximum HAGB fraction that can be attained during the entire process but also the HAGB fraction that can be attained at every strain level. It can be conjectured that p_L is a material-related parameter representing the material facility to attain HAGBs at a given strain.

The results in Fig. 5(b) show that for all studies alloys the entropy grows to a maximum value and then decreases with accumulated strain. The entropy of Cu-2%Co decreases most rapidly and approaches a value close to half of the maximum entropy at $\varepsilon = 12$. The entropy of oxygen-free Cu and Cu-0.1%Cr-0.06%Zr maintain large values after the maximum value, which means a richer variety of TJ types exist in these configurations compared to the other two materials.

4.2. HPT processing of copper alloys

HPT applies substantial pressure (typically about 1–6 GPa) to the circular surface of a thin disk and then rotates the anvil to induce shear strain. The method results in a significantly uneven distribution of plastic strain along the sample radius and is limited to small samples [14]. The equivalent strain varies significantly with distance from the centre of the disc. For an ideal rigid cylinder, the shear strain by HPT can be calculated from the equation:

$$\gamma = \frac{2\pi N r}{h}, \tag{16}$$

where N is the number of revolutions, r is the distance from the centre of the disk, and h is the thickness of the specimens, respectively. This is only valid if no thickness changes occur. The equivalent plastic strain, conjugate to the von Mises equivalent stress, is:

$$\varepsilon_N = \frac{\gamma}{\sqrt{3}} = \frac{2\pi N r}{\sqrt{3}h}. \tag{17}$$

The discrete model for HPT considers a radial section tessellated into cells similar to the ECAP model, as shown in Fig. 6. The computational section has a length of 5 mm, the right end of the section, with a section-based coordinate $x = 0$ mm at a distance $a > 0$ mm from the centre of the physical disk. The section is divided into five groups, as shown in Fig. 6. Each group is formed by the grain boundaries with x coordinates of their centres in the intervals (with unit mm): $[0, 1)$, $[1, 2)$, $[2, 3)$, $[3, 4)$, $[4, 5]$. In such case, $\varepsilon_N = \frac{2\pi N r}{\sqrt{3}h} = \frac{2\pi}{\sqrt{3}h} \cdot N \cdot r = m \cdot N \cdot r$ for each grain boundary, where $r = a+x$, the thickness $h = 0.8$mm [71–73]. The number of grains in the disc model is 10 000, and 500 grains in the section (see Fig. 6), which is enough to show the local deformation behaviour for the HPT process. The fraction of HAGBs in one group shown in Fig. 6, circled in red, represents the half-radius to the centre of the disk under the action of HPT, i.e. the fraction of HAGBs at a distance 0.25 mm from the disc centre.

Fig. 7(a) shows the experimental [71–73] (symbols) and calculated (curves) evolution of HAGBs fraction with accumulated strain for HPT-processed copper alloys Cu-0.17Zr, pure Cu, and Cu-Ni-Si. The curves are obtained by fitting the indicated Ising parameters. Fig. 7(b) shows the configuration entropy as a function of the accumulated strain.

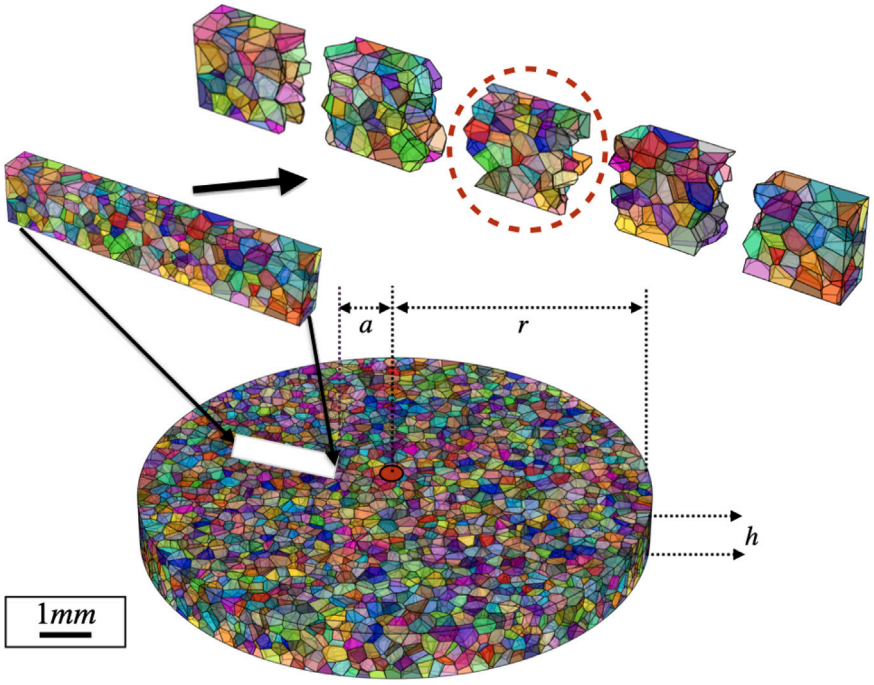

Fig. 6. The whole disc radial section is used for calculations and its division into five pieces.

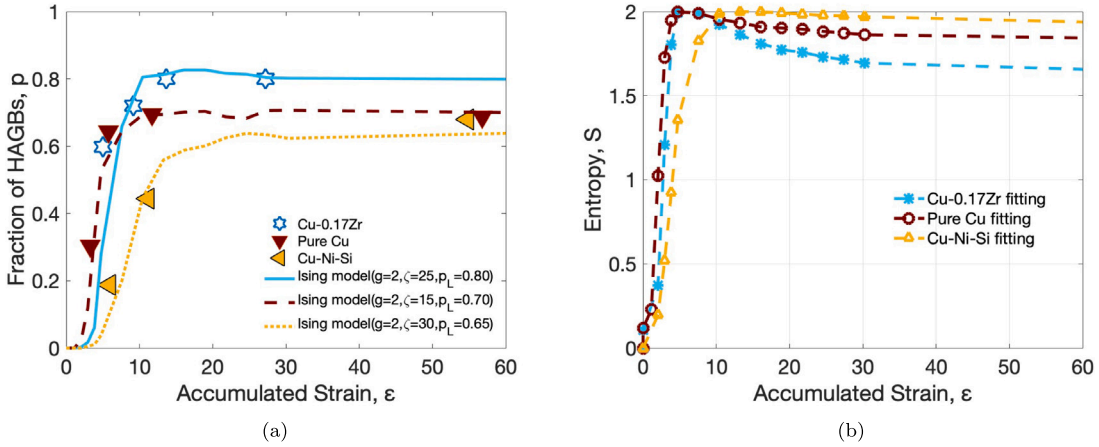

Fig. 7. (a) Comparison of the simulation curve for HAGBs fraction evolution with the experimental data on HPT processed copper alloys Cu-0.17Zr [71], Pure Cu [72], Cu-Ni-Si [73]; (b) Configurational TJs entropy as function to the accumulated plastic strain during HPT.

The parameter g acts on the interaction term in the Hamiltonian, Eq. (4). It can be seen in Fig. 7(a) that the HPT process requires a larger g than the ECAP process (Fig. 5(a)). It can be concluded that g is dictated by the experimental procedure. The parameter ζ acts on both terms in the Hamiltonian. Both Figs. 5(a) and 7(a) show that larger values of ζ yield slower growth of HAGB fraction with plastic strain.

The results in Fig. 7(b) show that the for all studies alloys the entropy grows to a maximum value, however, unlike the ECAP-processed alloys and the entropy decrease is negligible. This means that the HTP-process maintains the highest diversity of TJs subsequently.

4.3. Comparison with other conversion strategies

Previously investigated strategies for conversion between LAGBs and HAGBs included conversion of randomly selected grain boundaries (random) and conversion producing maximum increase of the configurational entropy (maximum entropy production, or MEPP) [45]. The results of these studies are compared with the results from the present work in terms of entropy dependence on HAGBs fraction in Fig. 8.

The results of the Ising-like model applied to ECAP correspond well to the strategy with random conversion and are lower than the MEPP results. Contrarily, the HPT appears to be most closely represented by the MEPP model. This suggests that the addition of strain gradient may have an effect similar to MEPP for the evolution process. It also indicates higher deviation from equilibrium process states, which the MEPP strategy commonly describes.

5. Discussion and conclusions

The defect structure evolution during different processing routes of copper alloys can lead to very different microstructures. The fraction of defects and their mutual arrangement (topology of their network) affect most of the physical and mechanical properties of materials. Experimental characterisations providing the texture (grain crystallographic orientations) and the fractions of various defect types are common. However, studies of spatial defect arrangements remain relatively rare due to the lack of appropriate discrete models involving thermodynamics and multi-dimensional features in the defect structure evolution

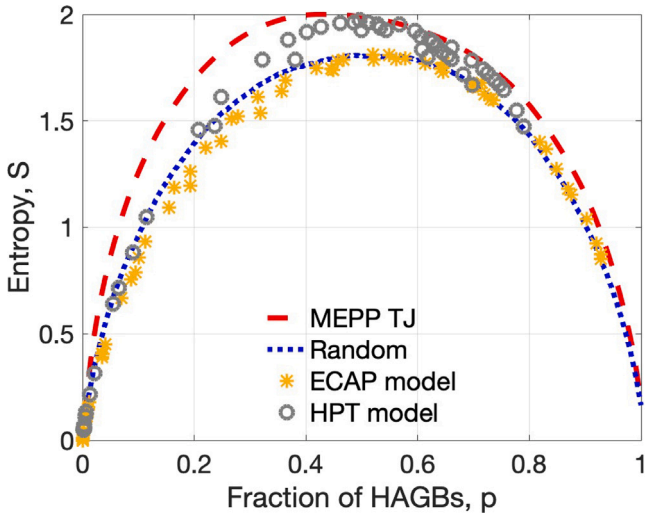

Fig. 8. Configuration entropy [45] with different evolution strategies.

process. This often leads to superficial comparisons of different microstructures when two structures are stated to be similar only because of the visual resemblance in their texture or equal defect fractions.

Grain boundary network evolution during the CDRX processes, dominant at low-temperature SPD processing routes like ECAP, has been the focus of this work. CDRX is characterised by the formation of new, smaller grains due to an increase in sub-boundary misorientations caused by the continuous accumulation of dislocations introduced by the deformation. An element of this process is the conversion of initial LAGBs into HAGBs. A significant amount of extraordinary mechanical properties of metallic materials after SPD, e.g., functional properties such as electrical and magnetic, strongly depend on the amount and balance between LAGBs and HAGBs. The considered ECAP and HPT processing of copper alloys is a wide and promising area of engineering of bulk ultrafine-grained metals practical for the design of novel functional materials for electro-mechanical applications. Unfortunately, the research on the grain boundary networks forming during SPD is very limited to date.

Previous works [45,46] followed the approach by Frary and Schuh [22,51,74] to study grain boundary TJ networks and TJ types distributions during SPD of copper alloys. It was shown that their distribution for these alloys is neither random nor fibre textured [45], but rather close to what is produced by a process following the maximum entropy production principle [75]. The present work substantially enriches the analysis by employing a new Ising-like 3D model based on the energy minimisation principle and a detailed analysis of the topological evolution of HAGBs and related TJ networks. It is used for the first time to study evolution during CDRX. The relations between HAGB fractions and accumulated strains used in the analysis are based on experimental data from the literature and correspond to actual SPD processing routes. The energy minimisation model is shown to be helpful in predicting such functions.

On the other hand, materials with the same fractions of "special" grain boundaries can have largely topologically different grain boundary networks possessing various levels of meta-stability. Their evolution may be governed by different principles, such as energy minimisation (equilibrium processes) or maximum entropy production (highly non-equilibrium processes). Simulations reveal that a single "general" physical principle for microstructure evolution cannot provide a realistic description of microstructure development during SPD. The outcome, which requires further investigation and experimental validation, is that the relatively homogeneous deformation conditions (ECAP case) are most closely described by the results obtained with the minimum energy principle provided by the Ising-like model, while conditions with strong deformation gradient (HPT case) appear to be close to the results obtained with the maximum entropy production principle. Clarifying such points might reveal the principal differences in structure evolution in the presence of a strong deformation gradient.

It is anticipated that this work will precipitate the development of advanced discrete models for grain boundary engineering, including multi-states and cluster models, delivering further information on grain boundary networks and allowing more accurate controls of the grain boundary evolution process.

CRediT authorship contribution statement

Siying Zhu: Conceptualization, Data curation, Formal analysis, Investigation, Methodology, Resources, Software, Validation, Visualization, Writing – original draft, Funding acquisition. **Elijah Borodin:** Conceptualization, Data curation, Formal analysis, Funding acquisition, Project administration, Supervision, Writing – review & editing, Methodology. **Andrey P. Jivkov:** Conceptualization, Funding acquisition, Project administration, Supervision, Writing – review & editing.

Declaration of competing interest

The authors declare that they have no known competing financial interests or personal relationships that could have appeared to influence the work reported in this paper.

Data availability

Data will be made available on request.

Acknowledgements

Zhu acknowledges gratefully the financial support of the China Scholarship Council and the University of Manchester via the joint PhD scholarship programme. Borodin and Jivkov acknowledge the financial support from the Engineering and Physical Sciences Research Council (EPSRC) UK via grants EP/V022687/1 (PRISB) and EP/N026136/1 (GEMS), respectively.

The authors confirm that the data supporting the findings of this study is available within the article. More simulation data, including raw/processed data required to reproduce these findings, will be shared in the hosting http://materia.team/.

References

[1] V.M. Segal, Materials processing by simple shear, Mater. Sci. Eng. A 197 (2) (1995) 157–164.
[2] R.Z. Valiev, R.K. Islamgaliev, I.V. Alexandrov, Bulk nanostructured materials from severe plastic deformation, Prog. Mater. Sci. 45 (2) (2000) 103–189.
[3] A.P. Zhilyaev, G.V. Nurislamova, B.K. Kim, M.D. Baró, J.A. Szpunar, T.G. Langdon, Experimental parameters influencing grain refinement and microstructural evolution during high-pressure torsion, Acta Mater. 51 (3) (2003) 753–765.
[4] Taku Sakai, Andrey Belyakov, Rustam Kaibyshev, Hiromi Miura, John J. Jonas, Dynamic and post-dynamic recrystallization under hot, cold and severe plastic deformation conditions, 2014.
[5] Jiaxin Lv, Jing Hua Zheng, Victoria A. Yardley, Zhusheng Shi, Jianguo Lin, A review of microstructural evolution and modelling of aluminium alloys under hot forming conditions, Metals (Basel) 10 (11) (2020) 1–33.
[6] Y. Estrin, A. Vinogradov, Extreme grain refinement by severe plastic deformation: A wealth of challenging science, Acta Mater. 61 (3) (2013) 782–817.
[7] V.M. Segal, V.I. Reznikov, A.E. Dobryshevshiy, V.I. Kopylov, Plastic working of metals by simple shear, Russ. Metall. 1 (1981) 99–105.
[8] Anna Morozova, Elijah Borodin, Vladimir Bratov, Sergey Zherebtsov, Andrey Belyakov, Rustam Kaibyshev, Grain refinement kinetics in a low alloyed Cu-Cr-Zr alloy subjected to large strain deformation, Materials (Basel) 10 (12) (2017) 1394.
[9] P.W. Bridgman, Effects of high shearing stress combined with high hydrostatic pressure, Phys. Rev. 48 (10) (1935) 825–847.

[10] Georgy J. Raab, Ruslan Z. Valiev, Terry C. Lowe, Yuntian T. Zhu, Continuous processing of ultrafine grained Al by ECAP-conform, Mater. Sci. Eng. A 382 (1–2) (2004) 30–34.

[11] Anna Bodyakova, Maksim Tkachev, Georgy I. Raab, Rustam Kaibyshev, Andrey N. Belyakov, Regularities of microstructure evolution in a Cu-Cr-Zr alloy during severe plastic deformation, Materials (Basel) 15 (16) (2022) 5745.

[12] Olga Shakhova, Neural crest stem cells in melanoma development, Curr. Opin. Oncol. 26 (2) (2014) 215–221.

[13] Erell Bonnot, Anne Laure Helbert, François Brisset, Thierry Baudin, Microstructure and texture evolution during the ultra grain refinement of the armco iron deformed by accumulative roll bonding (ARB), Mater. Sci. Eng. A 561 (2013) 60–66.

[14] Kaveh Edalati, Zenji Horita, A review on high-pressure torsion (HPT) from 1935 to 1988, Mater. Sci. Eng. A 652 (2016) 325–352.

[15] Irene J. Beyerlein, László S. Tóth, Texture evolution in equal-channel angular extrusion, 2009.

[16] K. Huang, R.E. Logé, A review of dynamic recrystallization phenomena in metallic materials, 2016.

[17] S. Gourdet, F. Montheillet, A model of continuous dynamic recrystallization, Acta Mater. 51 (9) (2003) 2685–2699.

[18] E.N. Borodin, A. Morozova, V. Bratov, A. Belyakov, A.P. Jivkov, Experimental and numerical analyses of microstructure evolution of Cu-Cr-Zr alloys during severe plastic deformation, Mater. Charact. 156 (2019) 109849.

[19] Louisette Priester, Grain Boundaries: From Theory to Engineering, Vol. 172, Springer, 2013, pp. 217–240.

[20] B. Bay, N. Hansen, D.A. Hughes, D. Kuhlmann-Wilsdorf, Overview no. 96 evolution of f.c.c. deformation structures in polyslip, Acta Metall. Mater. 40 (2) (1992) 205–219.

[21] F.J. Humphreys, M. Hatherly, Recrystallization and Related Annealing Phenomena, Elsevier, 2012, pp. 1–497.

[22] M. Frary, C.A. Schuh, Connectivity and percolation behaviour of grain boundary networks in three dimensions, Phil. Mag. 85 (11) (2005) 1123–1143.

[23] Håkan Hallberg, Approaches to modeling of recrystallization, Metals (Basel) 1 (1) (2011) 16–48.

[24] Jaspreet S. Nagra, Abhijit Brahme, Julie Lévesque, Raja Mishra, Ricardo A. Lebensohn, Kaan Inal, A new micromechanics based full field numerical framework to simulate the effects of dynamic recrystallization on the formability of HCP metals, Int. J. Plast. 125 (2020) 210–234.

[25] P. Germain, Q.S. Nguyen, P. Suquet, Continuum thermodynamics, J. Appl. Mech. Trans. ASME 50 (4) (1983) 1010–1020.

[26] H.R. Shercliff, A.M. Lovatt, Modelling of microstructure evolution in hot deformation, Philos. Trans. R. Soc. Lond. Ser. A Math. Phys. Eng. Sci. 357 (1756) (1999) 1621–1643.

[27] Alexei Vinogradov, Yuri Estrin, Analytical and numerical approaches to modelling severe plastic deformation, Prog. Mater. Sci. 95 (2018) 172–242.

[28] V. Bratov, E.N. Borodin, Comparison of dislocation density based approaches for prediction of defect structure evolution in aluminium and copper processed by ECAP, Mater. Sci. Eng. A 631 (2015) 10–17.

[29] Elijah N. Borodin, Alexander E. Mayer, Influence of structure of grain boundaries and size distribution of grains on the yield strength at quasistatic and dynamical loading, Mater. Res. Express 4 (8) (2017) 085040.

[30] Esteban P. Busso, A continuum theory for dynamic recrystallization with microstructure-related length scales, Int. J. Plast. 14 (4–5) (1998) 319–353.

[31] C.M. Sellars, Q. Zhu, Microstructural modelling of aluminium alloys during thermomechanical processing, Mater. Sci. Eng. A 280 (1) (2000) 1–7.

[32] Elijah Borodin, Andrey P. Jivkov, Alexander G. Sheinerman, Mikhail Yu Gutkin, Optimisation of rGO-enriched nanoceramics by combinatorial analysis, Mater. Des. 212 (2021) 110191.

[33] Peter A. Cundall, Otto D.L. Strack, A discrete numerical model for granular assemblies, Geotechnique 29 (1) (1979) 47–65.

[34] OTIS R. Walton, Explicit Particle-Dynamics Model for Granular Materials, Technical Report, Lawrence Livermore National Lab., CA (USA), 1982.

[35] A.D. Rollett, Overview of modeling and simulation of recrystallization, Prog. Mater. Sci. 42 (1–4) (1997) 79–99.

[36] Mark A. Miodownik, A review of microstructural computer models used to simulate grain growth and recrystallisation in aluminium alloys, J. Light Met. 2 (3 SPEC.) (2002) 125–135.

[37] Koenraad, et al., Computational Materials Engineering: An Introduction to Microstructure Evolution, Academic Press, 2010, p. 360.

[38] Koenraad G.F. Janssens, Random grid, three-dimensional, space-time coupled cellular automata for the simulation of recrystallization and grain growth, Modelling Simul. Mater. Sci. Eng. 11 (2) (2003) 157–171.

[39] S.P.A. Gill, A.C.F. Cocks, A variational approach to two dimensional grain growth - II. Numerical results, Acta Mater. 44 (12) (1996) 4777–4789.

[40] D. Weygand, Y. Bréchet, J. Lépinoux, A vertex dynamics simulation of grain growth in two dimensions, Philos. Mag. B Phys. Condens. Matter; Stat. Mech. Electron. Opt. Magn. Prop. 78 (4) (1998) 329–352.

[41] R. Loge, M. Bernacki, H. Resk, L. Delannay, H. Digonnet, Y. Chastel, T. Coupez, Linking plastic deformation to recrystallization in metals using digital microstructures, Phil. Mag. 88 (30–32) (2008) 3691–3712.

[42] M. Bernacki, R.E. Logé, T. Coupez, Level set framework for the finite-element modelling of recrystallization and grain growth in polycrystalline materials, Scr. Mater. 64 (6) (2011) 525–528.

[43] I. Steinbach, F. Pezzolla, B. Nestler, M. Seeßelberg, R. Prieler, G.J. Schmitz, J.L.L. Rezende, A phase field concept for multiphase systems, Phys. D 94 (3) (1996) 135–147.

[44] Long Qing Chen, Phase-field models for microstructure evolution, Annu. Rev. Mater. Sci. 32 (1) (2002) 113–140.

[45] Siying Zhu, Elijah Borodin, Andrey P. Jivkov, Triple junctions network as the key pattern for characterisation of grain structure evolution in metals, Mater. Des. 198 (2021) 109352.

[46] E.N. Borodin, A.P. Jivkov, Evolution of triple junctions' network during severe plastic deformation of copper alloys–a discrete stochastic modelling, Phil. Mag. 100 (4) (2020) 467–485.

[47] Romain Quey, Neper, 2021, URL https://neper.info/index.html.

[48] D. Rabbe, Computer simulations in materials science: the simulation of materials microstructure and properties, 2004.

[49] Franz Aurenhammer, Rolf Klein, Der-Tsai Lee, Voronoi Diagrams and Delaunay Triangulations, World Scientific Publishing Company, 2013.

[50] Nicholas Metropolis, Arianna W. Rosenbluth, Marshall N. Rosenbluth, Augusta H. Teller, Edward Teller, Equation of state calculations by fast computing machines, J. Chem. Phys. 21 (6) (1953) 1087–1092.

[51] Megan Frary, Christopher A. Schuh, Percolation and statistical properties of low- and high-angle interface networks in polycrystalline ensembles, Phys. Rev. B 69 (13) (2004) 134115.

[52] Sergey G. Abaimov, Statistical Physics of Non-Thermal Phase Transitions: From Foundations to Applications, Springer, 2015, p. 504.

[53] Stephen G. Brush, History of the Lenz-ising model, Rev. Modern Phys. 39 (4) (1967) 883–893.

[54] Barry A. Cipra, An introduction to the ising model, Am. Math. Mon. 94 (10) (1987) 937.

[55] W. Lenz, Beiträge zum verständnis der magnetischen eigenschaften in festen körpern., Phys. Z. 21 (1920) 613–615.

[56] Ernst Ising, Beitrag zur theorie des ferromagnetismus, Z. Phys. 31 (1) (1925) 253–258.

[57] James P. Sethna, Statistical Mechanics Entropy, Order Parameters and Complexity, Oxford University Press, 2006.

[58] A. Mishra, B.K. Kad, F. Gregori, M.A. Meyers, Microstructural evolution in copper subjected to severe plastic deformation: Experiments and analysis, Acta Mater. 55 (1) (2007) 13–28.

[59] E.N. Borodin, A.E. Mayer, M. Yu Gutkin, Coupled model for grain rotation, dislocation plasticity and grain boundary sliding in fine-grained solids, Int. J. Plast. 134 (2020) 102776.

[60] Charles Kittel, Paul McEuen, Kittel's Introduction to Solid State Physics, John Wiley & Sons, 2018.

[61] R. Robin Forman, Bochner's method for cell complexes and combinatorial Ricci curvature, Discrete Comput. Geom. 29 (3) (2003) 323–374.

[62] Edward Bormashenko, Mark Frenkel, Alla Vilk, Irina Legchenkova, Alexander A. Fedorets, Nurken E. Aktaev, Leonid A. Dombrovsky, Michael Nosonovsky, Characterization of self-assembled 2D patterns with voronoi entropy, Entropy 20 (12) (2018).

[63] Elijah N. Borodin, Alexander E. Mayer, Theoretical interpretation of abnormal ultrafine-grained material deformation dynamics, Modelling Simul. Mater. Sci. Eng. 24 (2) (2016) 025013.

[64] Niels Hansen, Hall-petch relation and boundary strengthening, Scr. Mater. 51 (8 SPEC. ISS.) (2004) 801–806.

[65] E.N. Borodin, V. Bratov, Non-equilibrium approach to prediction of microstructure evolution for metals undergoing severe plastic deformation, Mater. Charact. 141 (2018) 267–278.

[66] Megan E. Frary, Christopher A. Schuh, Correlation-space description of the percolation transition in composite microstructures, Phys. Rev. E 76 (4) (2007).

[67] Ruslan Z. Valiev, Terence G. Langdon, Principles of equal-channel angular pressing as a processing tool for grain refinement, Prog. Mater. Sci. 51 (7) (2006) 881–981.

[68] J. Dvorak, P. Kral, M. Svoboda, M. Kvapilova, V. Sklenicka, Enhanced creep properties of copper and its alloys processed by ECAP, in: IOP Conf. Ser. Mater. Sci. Eng., vol. 63, IOP Publishing, 2014, p. 12141.

[69] Peter Minárik, Tomáš Krajňák, Ondřej Srba, Jakub Čížek, Jenő Gubicza, Milan Dopita, Radomír Kužel, Miloš Janeček, Mechanical properties and microstructure development in ultrafine-grained materials processed by equal-channel angular pressing, Sev. Plast. Deform. Tech. (2017) 39–72.

[70] Meshal Y. Alawadhi, Shima Sabbaghianrad, Ying Chun Wang, Yi Huang, Terence G. Langdon, Characteristics of grain refinement in oxygen-free copper processed by equal-channel angular pressing and dynamic testing, Mater. Sci. Eng. A 775 (2020) 138985.

[71] Aicha Loucif, Thierry Baudin, François Brisset, Roberto B Figueiredo, Rafik Chemam, Terence G Langdon, An investigation of microtexture evolution in an AlMgSi alloy processed by high-pressure torsion, in: Mater. Sci. Forum, 702, Trans Tech Publ, 2012, pp. 165–168.

[72] Yi Huang, Shima Sabbaghianrad, Abdulla I. Almazrouee, Khaled J. Al-Fadhalah, Saleh N. Alhajeri, Terence G. Langdon, The significance of self-annealing at room temperature in high purity copper processed by high-pressure torsion, Mater. Sci. Eng. A 656 (2016) 55–66.

[73] Abdel Yazid Khereddine, Fayçal Hadj Larbi, Hiba Azzeddine, Thierry Baudin, François Brisset, Anne Laure Helbert, Marie Hélène Mathon, Megumi Kawasaki, Djamel Bradai, Terence G. Langdon, Microstructures and textures of a Cu-Ni-Si alloy processed by high-pressure torsion, J. Alloys Compd. 574 (2013) 361–367.

[74] Megan Frary, Christopher A. Schuh, Grain boundary networks: Scaling laws, preferred cluster structure, and their implications for grain boundary engineering, Acta Mater. 53 (16) (2005) 4323–4335.

[75] Leonid M. Martyushev, Vladimir D. Seleznev, Maximum entropy production principle in physics, chemistry and biology, Phys. Rep. 426 (1) (2006) 1–45.